

Calculation of intervalley scattering rates in $\text{Al}_x\text{Ga}_{1-x}\text{As}$: Effects of alloy and phonon scattering

C. H. Grein,* S. Zollner,[†] and M. Cardona

Max-Planck-Institut für Festkörperforschung, Heisenbergstrasse 1, D-7000 Stuttgart 80, Federal Republic of Germany

(Received 10 December 1990)

The lifetime broadening of an electron at the bottom of the Γ conduction-band valley in $\text{Al}_x\text{Ga}_{1-x}\text{As}$ is calculated for $0 \leq x \leq 1$. The parameter-free calculations take into account both electron-alloy scattering and electron-phonon scattering, with realistic models for the electronic band structures and phonon spectra. Second-order perturbation theory and the coherent-potential approximation are employed to evaluate the broadening. Intervalley scattering dominates the contributions to the lifetime in indirect-gap $\text{Al}_x\text{Ga}_{1-x}\text{As}$ ($x \geq 0.45$). The calculations give a fastest intervalley scattering time at temperature 10 K of 16 fs at $x=0.81$, with approximately twice as many transfers going to the L valleys as to the X valleys. Results are compared with lifetime broadenings obtained from spectroscopic ellipsometry, time-resolved photoluminescence, and Raman measurements.

I. INTRODUCTION

Intervalley scattering of conduction-band electrons in semiconductors is one of the most important scattering processes from the point of view of device technology. With the application of high electric fields, electrons in ordered or alloy semiconductors may scatter from the lowest point in the conduction band to higher-lying valleys. In general this transfer involves a change in the effective mass of the electron and thus in device performance. Resultant negative differential resistance in some semiconductors may be exploited to build Gunn diodes.¹ On the negative side, scattering to higher-effective-mass valleys will degrade the speed of ultrafast semiconductor devices,² or prevent the scattered electrons from contributing to lasing processes in semiconductor lasers.

Much effort has been invested in the study of intervalley scattering by phonons in ordered semiconductors; however, few detailed calculations in the technologically important ternary alloy $\text{Al}_x\text{Ga}_{1-x}\text{As}$ have been performed. Most work on electronic transport in semiconductor alloys has been performed using Monte Carlo simulations that employ only second-order perturbation theory in the electron-alloy and electron-phonon coupling strengths and may involve poor simplifying assumptions in the calculation of matrix elements and band structures in order to reduce computation time. We report here calculations that relax some of the usual assumptions and show where they are inadequate. Our results should serve as useful input parameters for future Monte Carlo simulations. $\text{Al}_x\text{Ga}_{1-x}\text{As}$ has been particularly intensively studied in the past decade for use in optoelectronic and fast electronic devices. In contrast with ordered crystals, alloy scattering inhibits electronic transport and is a significant mechanism for inducing intervalley transfers.³ Here, we calculate the scattering rates for $\Gamma \rightarrow X, L$ valley transfers as a function of Al concentration x . Our calculations are parameter-free in the sense that no parameters exist that are adjusted to match observed scattering rates (the electronic band structure and

the phonon spectra of GaAs and AlAs are, though, obtained from parameter-containing models). In Sec. II several methods are discussed for evaluating the electron-alloy disorder and electron-phonon scattering contributions to the scattering rate, including second-order perturbation theory and the coherent-potential approximation. In Sec. III, a comparison is made with experimental data for the lifetime broadenings of E_0 excitons in $\text{Al}_x\text{Ga}_{1-x}\text{As}$.

II. THEORY AND CALCULATIONS

The general problem of the transport of a nonequilibrium and dense electron gas in a finite temperature alloy is very difficult to treat; however, the consideration of only intervalley scattering is a significant simplification. In this section we discuss many-body effects and several approaches for calculating the scattering rate.

An important point that must be considered is the question of whether weak-scattering or strong-scattering methods should be employed to treat the electron-alloy disorder and electron-phonon scattering. It has been argued⁴ that the comparatively high mobility of electrons in $\text{Al}_x\text{Ga}_{1-x}\text{As}$ is an indication that only weak-scattering takes place (this is mainly a probe of intravalley-scattering strengths). Moreover, studies of nonequilibrium LO phonon distributions generated by means of hot-electron relaxation⁵ indicate that the Raman-active (zone-center) LO phonons in $\text{Al}_x\text{Ga}_{1-x}\text{As}$ are not localized and have well-defined wave vectors. Thus we adopt a weak-scattering formalism, and for electron-alloy disorder scattering compare results obtained from second-order perturbation theory with higher-order perturbation effects and the coherent-potential approximation in order to determine the strength of multiple-scattering corrections. In fact, the concept of intervalley scattering would be ill defined in the strong-scattering case because the Bloch electron index k would no longer be a quantum number. For electron-phonon scattering, only lowest-order perturbation theory is considered due to the com-

paratively weak deformation-potential electron-phonon coupling. Raman spectra^{6,7} reveal no structure beyond the allowed optical phonon modes and the disorder-activated acoustic and optical modes. We interpret this as an indication that clustering effects are weak in $\text{Al}_x\text{Ga}_{1-x}\text{As}$, and thus assume a random distribution of Al and Ga atoms on the cation sites in an otherwise perfect crystal.

Strong electric fields or optical excitation by means of a laser may result in the creation of a nonequilibrium population of carriers. If the time scale for the internal carrier equilibration due to electron-electron and electron-hole scattering is shorter than the time scale for alloy- and phonon-induced intervalley scattering, one can assume that the carriers are in internal equilibrium although they are not necessarily in equilibrium with the lattice. Under such circumstances one can employ the "temperature model" by assigning the electronic distribution an effective temperature T^* and the lattice a temperature T . The calculations presented here can be used to establish the validity of the temperature model for various composition ratios x by comparing the intervalley-scattering times to the internal carrier equilibration times.

The presence of a dense electron gas will produce a many-body renormalization of the phonons, which may result in the phonon spectral function displaying additional branches.⁸ However, in semiconductors, this renormalization is typically only significant for phonons with wave vectors extending over less than $\frac{1}{10} - \frac{1}{5}$ of the Brillouin zone.⁹ Thus, for electron-scattering from the Γ to the X or L valleys involving only a single phonon, this phonon will be essentially unrenormalized. For large Al concentration, the Γ valley lies quite high and some single-scattering events may involve smaller wave-vector-renormalized phonons, but the dominant contributions continue to involve only large crystal momentum changes. Scattering paths involving several small wave-vector phonons are less probable due to the weak electron-phonon coupling, and will be further weakened by free carrier screening of the deformation potential.⁹ Since we treat phonon-induced intervalley scattering by means of lowest-order perturbation theory, we do not consider the effects of screening of the phonons. Only the deformation-potential electron-phonon coupling needs to be considered, since the long-range Fröhlich and piezoelectric interactions are negligible for the large wave vectors needed for intervalley transfers.

Electron-electron and electron-hole scattering are unlikely to provide the large wave vectors necessary to induce intervalley transfers, but the presence of an electron gas does lead to band-gap renormalization and may limit the available phase space of final states. The relative renormalization of the Γ - L and Γ - X valley minima is of the order of 10 meV in highly excited ($10^{18} - 10^{19}$ electrons cm^{-3}) $\text{Al}_x\text{Ga}_{1-x}\text{As}$,¹⁰ quite small, and below the accuracy of our calculated band structures; thus it is not incorporated into the calculations. Moreover, we restrict the calculations to experimental situations where negligible filling takes place in the X or L valleys (such as with weak laser pulse methods) so that the final-state phase space is not limited by band filling.

Our calculation concentrates on a treatment of the electron-alloy disorder and electron-phonon scattering as the mechanisms for inducing intervalley transfers. We first calculate the scattering rate by means of second-order perturbation theory and later discuss multiple-scattering corrections. A good approach in an alloy is to treat scattering with respect to the virtual crystal (VC). Denoting the VC potential on the cation sites as $V_{\text{VC}} = xV_{\text{Al}} + (1-x)V_{\text{Ga}}$, where $V_{\text{Al}}(\mathbf{r})$ and $V_{\text{Ga}}(\mathbf{r})$ are the electronic potentials of Al and Ga, respectively, gives the scattering potentials of the Al- or Ga-occupied sites

(a) $\Sigma = \text{---} \times \text{---} + \text{---} \times \text{---} + \text{---} \times \text{---} \times \text{---} + \text{---} \times \text{---} \times \text{---}$

(b) $\Sigma = \left(\text{---} \times \text{---} + \text{---} \times \text{---} \times \text{---} + \text{---} \times \text{---} \times \text{---} \times \text{---} + \dots \right) + \left(\text{---} \times \text{---} + \text{---} \times \text{---} \times \text{---} + \text{---} \times \text{---} \times \text{---} \times \text{---} + \dots \right)$

(c) $\Sigma = \left(\text{---} \times \text{---} + \text{---} \times \text{---} \times \text{---} + \text{---} \times \text{---} \times \text{---} \times \text{---} + \dots \right) + \left(\text{---} \times \text{---} + \text{---} \times \text{---} \times \text{---} + \text{---} \times \text{---} \times \text{---} \times \text{---} + \dots \right) + \left(\text{---} \times \text{---} \times \text{---} + \text{---} \times \text{---} \times \text{---} \times \text{---} + \dots \right)$

(d) $\text{---} = \text{---} + \text{---} \text{---} \Sigma \text{---}$

(e) $\text{---} \times \text{---} \times \text{---}$

FIG. 1. Electronic self-energies with respect to the virtual-crystal energies due to alloy scattering in $\text{Al}_x\text{Ga}_{1-x}\text{As}$ in (a) first- and second-order perturbation theory (first-order contributions cancel); (b) T matrix approximation as discussed in text (no multiple-occupancy corrections); and (c) coherent-potential approximation. The solid lines represent the unperturbed Bloch electron propagators; in (a) and (b) a \times above a propagator represents x times the difference between the Al and virtual crystal potentials, a \times below a propagator represents $1-x$ times the difference between the Ga and virtual-crystal potentials; in (c) the \times 's are weighted by $P_s(x)$ rather than x above the propagator and $P_s(1-x)$ rather than $1-x$ below the propagator, where s is the number of interaction lines entering the \times (P_s is defined in Ref. 61); the double solid lines represent self-consistent insertions of the full electron propagators; and the dashed lines represent elastic scattering events. The final set of terms in (c) represents further multiple-occupancy corrections in the notation of Ref. 62. (d) is Dyson's equation for the full electron propagator. (e) is an example of low-order diagram not included in the coherent-potential approximation. The lifetime broadening is given by $\Gamma_{\text{el-dis}} = -\text{Im} \Sigma$.

$$\begin{aligned} V_{\text{Al,VC}} &= V_{\text{Al}} - V_{\text{VC}} = (1-x)(V_{\text{Al}} - V_{\text{Ga}}), \\ V_{\text{Ga,VC}} &= V_{\text{Ga}} - V_{\text{VC}} = -x(V_{\text{Al}} - V_{\text{Ga}}). \end{aligned} \quad (2.1)$$

$$\begin{aligned} \frac{N}{2} [x|V_{\text{Al,VC}}|^2 + (1-x)|V_{\text{Ga,VC}}|^2] \\ = \frac{N}{2} x(1-x)|V_{\text{Al}} - V_{\text{Ga}}|^2, \end{aligned} \quad (2.2)$$

The average of the squared scattering potential is therefore

where N is the number of lattice sites in the VC, and thus the first Born approximation for the elastic-scattering rate of an electron gas may be written as

$$\frac{1}{\tau} \equiv \frac{2\Gamma_{\text{el-dis}}}{\hbar} = \frac{N\pi}{\hbar} \sum_{i,f} e^{-\beta^*(E_i - E_0)} |\langle n_i \mathbf{k}_i | V_{\text{Al}}(\mathbf{r}) - V_{\text{Ga}}(\mathbf{r}) | n_f \mathbf{k}_f \rangle|^2 x(1-x) \delta(E_i - E_f) / Z, \quad (2.3)$$

where $Z = \sum_i e^{-\beta^*(E_i - E_0)}$; $\beta^* = 1/k_B T^*$; T^* is the temperature of the electron gas; E_i, E_f are the energies of initial occupied and final unoccupied Bloch states $|n_i \mathbf{k}_i\rangle$ and $|n_f \mathbf{k}_f\rangle$; E_0 is the electronic energy at the bottom of the Γ valley; and $\Gamma_{\text{el-dis}}$ is the lifetime broadening. This expression incorporates a thermal distribution for electrons, but any appropriate distribution may be used. A diagrammatic representation of Eq. (2.3) is shown in Fig. 1(a). In GaAs and AlAs the recombination lifetime is much longer than the intervalley-scattering time; thus the dominant contributions to the lifetime broadening come from intra- and intervalley scattering. In the absence of final-state damping¹¹ one may compare $\Gamma_{\text{el-dis}}$ (plus the smaller contributions of electron-phonon scattering) directly with measured linewidths. Thus the main assumptions of our calculations that limit the measured linewidths to which they can be directly compared are the absence of final-state filling and damping, and inhomogeneous broadening effects (see Sec. III).

We have evaluated Eq. (2.3) for the special case of a single initial state consisting of an electron at the bottom of the Γ valley; thus contributions to the scattering rate

will arise only from intervalley-scattering processes. The band structure and wave vectors were obtained in the VC approximation from local empirical pseudopotentials, with a basis of 89 plane waves (see also Refs. 12–16). The scattering potential $V_{\text{Al}}(\mathbf{r}) - V_{\text{Ga}}(\mathbf{r})$ was taken to be the difference between the pseudopotentials of the Al and Ga atoms. In earlier calculations, the simplifying assumptions of δ -function^{17,18} or square-well^{19–21} scattering potentials have been made, but we employ the physically more realistic pseudopotential scattering potential. Moreover, most earlier approaches assume a momentum-transfer independent matrix element,^{20–21} valid for small momentum transfers, and thus limit their applicability to intravalley scattering. Here, we evaluate the matrix elements in Eq. (2.3) exactly.

In terms of the plane-wave expansion of the Bloch function

$$|n\mathbf{k}\rangle = \frac{1}{\sqrt{V}} \sum_{\mathbf{G}} c_{n\mathbf{k}}(\mathbf{G}) \exp[i(\mathbf{k} + \mathbf{G}) \cdot \mathbf{r}], \quad (2.4a)$$

where V is the volume of the VC,

$$\begin{aligned} \langle n_i \mathbf{k}_i | V_{\text{Al}}(\mathbf{r}) - V_{\text{Ga}}(\mathbf{r}) | n_f \mathbf{k}_f \rangle \\ = \frac{1}{2N} \sum_{\mathbf{G}, \mathbf{G}'} c_{n_i \mathbf{k}_i}^*(\mathbf{G}) [\tilde{V}_{\text{Al}}(\mathbf{k}_i - \mathbf{k}_f + \mathbf{G} - \mathbf{G}') - \tilde{V}_{\text{Ga}}(\mathbf{k}_i - \mathbf{k}_f + \mathbf{G} - \mathbf{G}')] c_{n_f \mathbf{k}_f}(\mathbf{G}') e^{-i(\mathbf{k}_i - \mathbf{k}_f + \mathbf{G} - \mathbf{G}') \cdot \boldsymbol{\gamma}}, \end{aligned} \quad (2.4b)$$

where $\boldsymbol{\gamma} = a(1, 1, 1)/8$ is a cation site in a bond-centered coordinate system, and a is the lattice constant. Several sets of pseudopotential form factors have been developed for GaAs and AlAs.^{22–24} We employ those of Caruthers and Lin-Chung²² since they give good band structures for GaAs and AlAs (see Table I) compared with experiment, provide a direct-indirect gap crossover of $\text{Al}_x\text{Ga}_{1-x}\text{As}$ at $x \approx 0.45$ in the VC band structure in agreement with experiment, and have the same form factors for the As atom in GaAs and AlAs. These pseudopotentials extrapolate to $\tilde{V}(0) = -2E_F/3$, where E_F is the Fermi energy of an electron gas of the same density as the valence elec-

trons; calculations indicate that results are insensitive to this choice of the lower limit of the form factors versus $\tilde{V}(0) = 0$. The data in Table I are given so that a correspondence can be made between the lifetime broadenings expressed in Fig. 2 as a function of x and the broadenings as a function of the relative positions of the Γ , X , and L valley minima. It also shows that elastic scattering from the lowest point in the Γ valley is only possible to other states in the lowest conduction band, since the next higher band remains above Γ_{1c} for all x . The sum over final states in Eqs. (2.3) was evaluated by means of the tetrahedron method²⁵ with a raster of 505

TABLE I. Calculated electronic energies in eV (relative to valence-band maximum) at the minima of the Γ , X , and L conduction-band valleys and at X_{3c} (next higher band at X) in GaAs and AlAs, employing the empirical pseudopotentials of Ref. 18. The valley energies in the virtual-crystal band structure of $\text{Al}_x\text{Ga}_{1-x}\text{As}$ for any x may be obtained by means of linear interpolation. Values in parentheses are the best combined theoretical and experimental values (at 0 K) adopted in Ref. 40.

Valley	GaAs	AlAs
Γ_{1c}	1.487 (1.52)	2.807 (2.90)
L_{1c}	1.776 (1.82)	2.488 (2.48)
X_{1c}	1.931 (1.98)	2.224 (2.24)
X_{3c}	2.382 (2.38)	2.942 (2.89)

\mathbf{k}_f points in an irreducible $\frac{1}{48}$ wedge of the Brillouin zone. The calculated alloy-disorder contribution to the intervalley-scattering rate is presented in Fig. 2 and marked with "alloy." The figure shows that the contributions of intervalley-alloy scattering only occur when $\text{Al}_x\text{Ga}_{1-x}\text{As}$ is indirect ($x \geq 0.45$); small contributions due to band tailing for $x \leq 0.45$ will be discussed later.

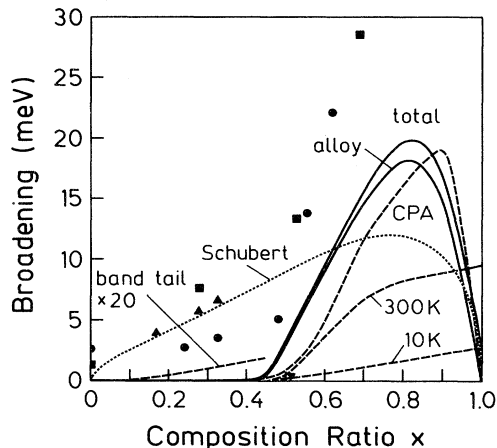


FIG. 2. Broadening of electronic states at the bottom of the Γ valley as a function of Al concentration in $\text{Al}_x\text{Ga}_{1-x}\text{As}$. The intervalley scattering rate for $x \geq 0.45$ is given by $\tau = \hbar / (2 \times \text{broadening})$. The solid line marked "alloy" gives the second-order perturbation-theory result for the broadening due to intervalley scattering induced by random, spatially extended alloy potentials. The dashed line marked "CPA" is an estimate of the same but employing the coherent-potential approximation with diagonal disorder only. The dashed lines marked "10 K" and "300 K" give the phonon-scattering contributions to the broadening at temperatures 10 and 300 K. The line marked "band tail" gives the alloy disorder contributions due to band tailing of the density of states. The line marked "total" is the sum of the "alloy," "band tail," and "10 K" lines. Individual points are values from photoluminescence (Ref. 59) (▲) at 4.8 K, spectroscopic ellipsometry (Ref. 59) (■) at 15 K, Raman (Ref. 60) (●) at 100 K measurements, and picosecond luminescence (Ref. 57) (▼) at 50 K. The dotted line marked "Schubert" is the calculated curve from Ref. 58.

For $0.45 \leq x \leq 0.51$ only scattering to the X valleys is energetically allowed, but contributions from scattering paths to the L valleys are permitted for large x . For $0.45 \leq x \leq 0.8$, the increasing density of final states dominates the increasing broadening, but for even larger x the decreasing alloy disorder dominates and leads to the vanishing of the broadening at $x = 1$. In Fig. 3 the contributions of $\Gamma \rightarrow X$ and $\Gamma \rightarrow L$ alloy-disorder scatterings are separated in order to establish the relative scattering strengths to the two valleys. The stronger contributions to the L valley relative to the X valley for $x \geq 0.8$ arise mainly from larger matrix elements, although they are also partially due to a greater density of final states.

Figure 3 also shows the alloy-disorder-induced scattering rate calculated by means of the commonly employed expression given in Refs. 20 and 21. To apply this expression to the present problem, two simplifying assumptions must be made. The X and L valleys are assumed to be parabolic, and the momentum transfer dependence of the matrix elements is neglected. Here, all input parameters were assumed to take their virtual crystal values.²⁶ As can be seen in Fig. 3, the simplified expression agrees well with our calculation for the peak scattering rate. However, due to neglect of the momentum transfer dependence of the matrix elements and the approximate nature of representation of the band structure, it incorrectly weights the relative $\Gamma \rightarrow X$ to $\Gamma \rightarrow L$ transfer rates, predicting for all x stronger scattering to the X valleys (this can be seen in Fig. 3 by the overall shift of the curve to lower x values with respect to the curve marked "sum").

In a manner analogous to the treatment of the electron-alloy-disorder scattering, the electron-phonon scattering contribution to the intervalley-scattering rate may be calculated in the first Born approximation. Most earlier approaches assume a momentum-independent deformation-potential interaction and parabolic valleys by employing Conwell's formula;²⁷ however, the need to take the momentum dependence into account has been

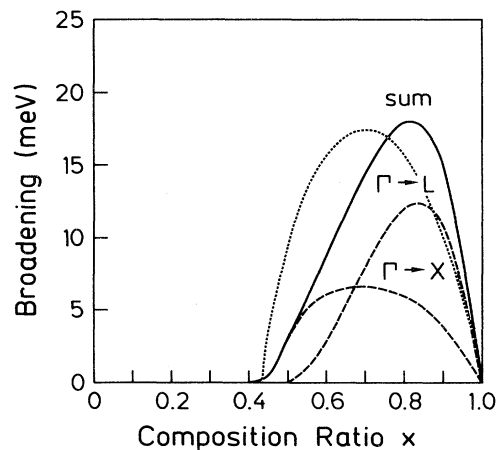


FIG. 3. Calculated lifetime broadenings due to electron-alloy disorder scattering in $\text{Al}_x\text{Ga}_{1-x}\text{As}$, showing separately the contributions of $\Gamma \rightarrow L$ and $\Gamma \rightarrow X$ valley transfers and their sum, marked "sum." The dotted line is the broadening calculated using the expression given in Ref. 20.

emphasized in Ref. 28. Thus we employ a method similar to that used in Ref. 28 for intervalley scattering in ordered III-V semiconductors, and only discuss here the differences due to the consideration of an alloy.

The phonon dispersion of $\text{Al}_x\text{Ga}_{1-x}\text{As}$ displays two-mode behavior,^{29,30} and has been calculated by a number of means including the coherent-potential approximation (CPA).^{31,32} We have employed the CPA (Refs. 33, 34) to calculate the alloy-disorder-induced corrections to the phonon frequencies of GaAs and AlAs, which were obtained from a shell model.³⁵ Our CPA method is the same as in Ref. 36, except that the analytic continuation scheme of Ref. 37 was employed to improve the convergence of the Green's function. The 14-shell-model parameters for GaAs were obtained from Ref. 38 and the same parameters, except for the replacement of the cation atomic mass, were used for AlAs. Recent density-functional calculations³⁹ and Raman measurements⁴⁰ support this "mass approximation" in obtaining the shell-model parameters of AlAs from those of GaAs. Large-wave-vector phonons are mainly responsible for intervalley transfers; however, extensive measurements of the composition dependence of phonon frequencies are only available for phonons near Γ ; thus, as a check, our calculations (CPA and shell model) are compared with phonon frequencies at Γ in Fig. 4. The figure also shows that the broadening (hatched area) of $\text{TO}(\Gamma)$ phonons is greater than that of $\text{LO}(\Gamma)$ phonons, a consequence of the greater density of states at energies near that of the $\text{TO}(\Gamma)$ branches. This is in agreement with recent supercell calculations;⁴¹ experimentally,^{42,43} $\text{LO}(\Gamma)$ phonons show broadenings of approximately 2 cm^{-1} for various alloy compositions. We have not found published measurements of the $\text{TO}(\Gamma)$ phonon broadenings. The CPA method cannot describe local phonon modes; thus the calculations for AlAs-like phonons for $x \approx 0$ are poor; also the CPA results may be poor for the strongly reso-

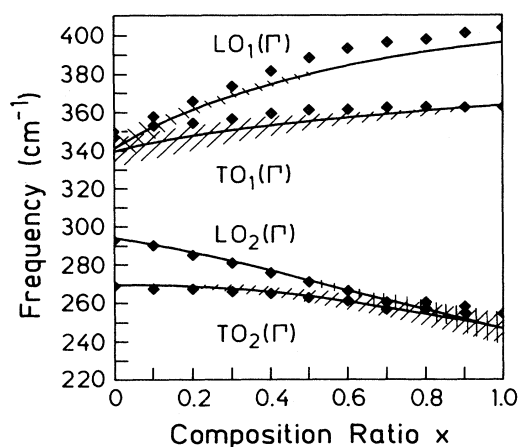


FIG. 4. Optical-phonon frequencies at Γ in $\text{Al}_x\text{Ga}_{1-x}\text{As}$ obtained (solid lines) from coherent-potential approximation corrections to shell-model calculations [showing AlAs-like modes (TO_1 , LO_1) and GaAs-like modes (TO_2 , LO_2)], compared with the measured points of Ref. 30. The width of the calculated lines give the alloy-disorder-induced broadening.

nant GaAs-like modes near $x \approx 1$. The scattering rate was evaluated in the Born approximation in the VC electronic band structure, including CPA corrections to all phonon frequencies on a raster of 505 q points in an irreducible $\frac{1}{48}$ wedge in the Brillouin zone, and is shown in Fig. 2 for temperatures of 10 and 300 K. Due to the inelastic nature of electron-phonon-scattering events, their contributions to the scattering rate become significant only for larger x than the contributions of elastic-alloy-disorder scattering events. The inelastic scattering rate for an electron initially at the bottom of the Γ valley may be written as²⁸

$$\frac{1}{\tau_{\text{el-ph}}(T)} = \frac{2}{\hbar} \int_0^\infty d\Omega g^2 B(\Omega) [N(\Omega) + \frac{1}{2}], \quad (2.5)$$

where $N(\Omega) = 1/[\exp(\Omega/k_B T) - 1]$ is the Bose function for the lattice temperature T , and $g^2 B(\Omega)$ is the electron-phonon spectral function. This expression takes into account both phonon emission and absorption processes. As can be seen from Eq. (2.5), at zero temperature the area under the spectral function is proportional to the scattering rate. Thus one can determine the relative contributions of the various phonon branches by examining the spectral function. At finite temperatures the Bose function will give the lower-energy modes more weight. The spectral function for several different alloy compositions is presented in Fig. 5.

As a check on our phonon-induced scattering rate, we fit Conwell's formula²⁷ to our 300-K scattering rate for

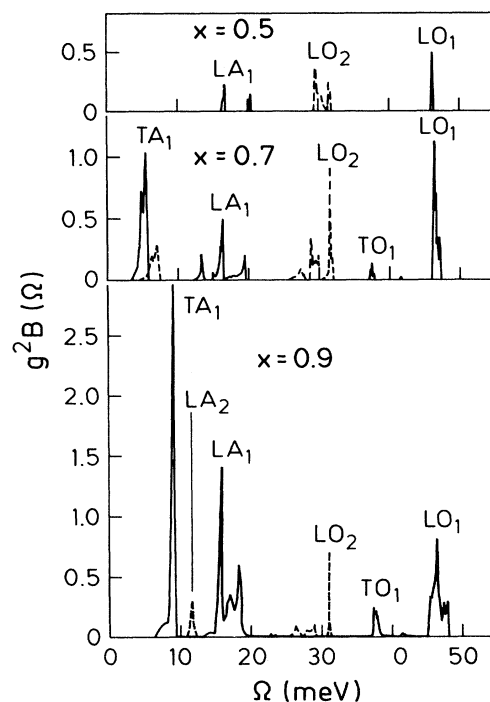


FIG. 5. Electron-phonon spectral function for various Al concentrations in $\text{Al}_x\text{Ga}_{1-x}\text{As}$, including coherent-potential approximation corrections to phonon frequencies. The GaAs-like mode contributions are shown with dashed lines and the AlAs-like mode contributions with solid lines.

$x = 1$ (pure AlAs), and obtain the physically reasonable value of 10 eV/Å for the intervalley deformation potential. This shows that our results are consistent with earlier, more approximate, methods for ordered semiconductors.

So far, only scattering within the VC electronic band structure has been considered. However, disorder modifies band structures beyond the virtual-crystal approximation. In a disordered material, the electronic wave vectors \mathbf{k} for extended states are no longer exact quantum numbers, the lack of exactness depending on the strength and density of the scattering potentials. Moreover, the density of extended states may be less than in the corresponding ordered crystal, with the missing states contributing to the formation of band tails of localized states within the gap.⁴⁴ Thus the density of states does not vanish at the mobility edge, which will be reflected in small contributions to the broadening. Precise calculations of this broadening are difficult to perform;⁴⁵ but they may be simply estimated by means of the self-consistent Born approximation:

$$\Gamma_{\text{el-dis}} \approx \pi |\langle \Gamma_c | H_{\text{scatt}} | \Gamma_c \rangle|^2 \text{Re} \rho(-i\Gamma_{\text{el-dis}}), \quad (2.6)$$

where H_{scatt} is the scattering Hamiltonian, Γ_c refers to the lowest VC conduction-band state at Γ , and $\rho(E)$ is the electronic density of states near the band edge. A diagrammatic representation of the self-consistent Born approximation is obtained from Fig. 1(a) by replacing the free-electron propagator with the full electron propagator. H_{scatt} may be estimated from Eq. (2.2), neglecting the smaller phonon contributions. By letting $|V_{\text{Al}} - V_{\text{Ga}}|$ be the difference between the average AlAs and GaAs antibonding energies,⁴⁶

$$|\langle \Gamma_c | H_{\text{scatt}} | \Gamma_c \rangle|^2 \approx x(1-x) |0.51|^2 \text{eV}^2.$$

The density of states may be estimated by the free-electron expression

$$\rho(E) = V(2m^*)^{3/2} E^{1/2} / [(2\pi)^2 \hbar^3],$$

where the effective mass is²⁶ $m^* = [0.067(1-x) + 0.150x]m_0$, the free-electron mass is m_0 , the volume of a unit cell is $V = a^3/4$, and the lattice constant approximated by the linear interpolation is $a = [(1-x)5.639 + x(5.669)] \text{Å}$. The broadenings obtained from Eq. (2.6) are displayed in Fig. 2 and are marked as "band tail." Equation (2.6) describes a Lorentzian decay of the band-tail density of states, which is an overestimate of the actual exponential decay. In Fig. 2 the band-tail broadening is plotted for $x \leq 0.45$; it indicates that this contribution to the total broadening is negligible.

We next discuss multiple-scattering contributions to the intervalley scattering rate within the VC approximation as a check on the accuracy of the second-order perturbation-theory results. The electron-phonon and electron-alloy-disorder interactions are only completely separable in second-order perturbation theory, however; for simplicity we only consider the electron-alloy disorder terms to higher orders. For a given type of scattering center, the T matrix defined by⁴⁷

$$T_{n\mathbf{k},n'\mathbf{k}'} = V_{n\mathbf{k},n'\mathbf{k}'} + \sum_{n''\mathbf{k}''} \frac{V_{n\mathbf{k},n''\mathbf{k}''} T_{n''\mathbf{k}'',n'\mathbf{k}'}}{E_{n\mathbf{k}} - E_{n''\mathbf{k}''} + i\delta}, \quad (2.7)$$

where $V_{n\mathbf{k},n'\mathbf{k}'} = \langle n\mathbf{k} | V_{\text{VC}} | n'\mathbf{k}' \rangle$, describes all multiple-scattering contributions from a single scattering center. In order to estimate multiple-scattering corrections to the intervalley scattering rate, Eq. (2.7) was evaluated for (n, \mathbf{k}) being the lowest VC conduction-band state at Γ , (n', \mathbf{k}') belonging to the lowest bands in the X and L valleys, and the pseudopotentials $V_{\text{VC}}(\mathbf{r}) = V_{\text{Al,VC}}(\mathbf{r})$ or $V_{\text{VC}}(\mathbf{r}) = V_{\text{Ga,VC}}(\mathbf{r})$. The broadening is given by $\Gamma_{\text{el-dis}} = -\text{Im}[xT_{\text{Al,VC}} + (1-x)T_{\text{Ga,VC}}]$, and is shown diagrammatically in Fig. 1(b). Extensions to this formalism, such as the addition of multiple-occupancy corrections (so that contributions due to, for example, Al and Ga atoms occupying the same site are eliminated) to obtain the well-known average T matrix approximation, are discussed in Ref. 48. We find that the magnitude of some of the T matrix elements may be as much as 7% larger than the magnitude of the corresponding lowest-order term elements ($V_{n\mathbf{k},n'\mathbf{k}'}$). This indicates that the second order in perturbation theory accounts for the bulk of the single-scattering-center contributions to the transition amplitude. Unfortunately, computational resources prevent us from evaluating Eq. (2.7) on a sufficiently dense grid of \mathbf{k} points in order to obtain accurate estimates of scattering rates, but we do obtain this approximation to the extent that Eq. (2.3) underestimates the scattering rate. A comparison of the virtual-crystal, second-order perturbation-theory-corrected, and CPA-corrected band structures of several other materials is made in Ref. 49.

We have exhausted our computational abilities to examine multiple scattering from spatially extended pseudopotentials. However, by considering only diagonal disorder⁴⁸ a significantly higher number of multiple-scattering contributions can be taken into account. One such approach is to evaluate the electronic-state broadening by means of the CPA. The imaginary part of the self-energy evaluated at the bottom of the Γ conduction-band valley gives an estimate of the lifetime broadening due to intervalley scattering. This method is impractical to apply for scattering from spatially extended pseudopotentials, although off-diagonal disorder can be partially incorporated by means of the molecular CPA,⁵⁰ and multiplicative off-diagonal disorder as discussed in Refs. 51 and 52. A simple form of the CPA by Chen and Sher⁴⁶ describes scattering from δ -function potentials (no off-diagonal disorder) equal to the average antibonding energies of the component compounds (GaAs and AlAs). By averaging over the antibonding states, different chemical origins of these states (such as s like and p like) and their different sensitivities to disorder are not taken into account, but the method does have the advantage of being very easy to apply. Earlier CPA calculations of the self-energy of electrons in $\text{Al}_x\text{Ga}_{1-x}\text{As}$ have been reported in Refs. 46 and 53; however, it is difficult to extract the broadenings at the bottom of the Γ valley from these papers. Therefore, we have employed the method of Ref. 46 to calculate the broadenings, except for using the density of states obtained by means of pseudopotential calcu-

lations, to obtain the scattering rates marked in Fig. 2 by "CPA." The CPA method includes contributions from the scattering by the full T matrix of each scattering center as well as some multiple-scattering paths involving return visits to a given scattering center [see Fig. 1(c)]. One can approximately account for the phonon contributions to the total self-energy by subtracting the phonon scattering self-energy in the denominator of the free-electron Green's function, as described in Ref. 54. We see in Fig. 2 that the CPA estimate of the scattering rate generally lies somewhat below that obtained by means of second-order perturbation theory. This may at first seem surprising, but can be understood to be due to the consideration of only diagonal disorder estimated by the difference in the component average antibonding energies in the CPA method, whereas the second-order perturbation-theory results include scattering from spatially extended potentials (pseudopotentials).

III. DISCUSSION AND SUMMARY

A comparison of the evaluated lifetime broadenings with measurements (Fig. 2) reveals that the calculation generally underestimates the broadenings over the entire composition range of $\text{Al}_x\text{Ga}_{1-x}\text{As}$. There is a tendency for experimental data to overestimate the broadening, as has been discussed for spectroscopic ellipsometry in Refs. 28 and 55, which may account in part for the discrepancy. The calculated values are also below the upper limits determined in Ref. 56 from picosecond luminescence measurements. A simple analysis of these measurements^{56,57} suggests that the alloy disorder contributions are a factor of 2 weaker than the phonon-scattering contributions, although a more thorough analysis of the data is needed. The lowest-order perturbation-theory results for the electron-phonon-scattering contributions should be accurate due to the weakness of the deformation-potential electron-phonon interaction; however, as discussed in the preceding section, multiple-scattering corrections to the electron-alloy disorder contributions will make up at least part of the difference, but it is difficult to estimate how much. Elements of the T matrix are as much as 7% larger in magnitude than the lowest-order terms; moreover, there are contributions from

scattering paths involving repeated scatterings from a given site that are not taken into account in the T matrix. The coherent-potential approximation calculations do take into account a large number of multiple-scattering corrections, but, due to neglect of off-diagonal disorder, give broadenings generally somewhat less than second-order perturbation theory. The calculated alloy disorder contributions might be reduced with the choice of different pseudopotential form factors.²³

We have considered homogeneous contributions to the linewidth broadening. An additional mechanism has been proposed⁵⁸ for inhomogeneous disorder contributions to the broadening. This involves the consideration of statistical fluctuations in the Al and Ga density within an excitonic orbit, with resultant real self-energy shifts contributing to the linewidth, in contrast with our consideration of a fixed Al and Ga distribution and only the imaginary self-energies of the electrons being important. It is interesting to note that the sum of our calculation and that of Ref. 58 (Fig. 2) gives a good fit to some of the observed broadenings; however, the method of Ref. 58 requires a more fundamental treatment of correlated electron-hole pairs and their broadening in order to be quantitatively verifiable.

In summary, we have performed detailed calculations of intervalley scattering rates in $\text{Al}_x\text{Ga}_{1-x}\text{As}$ alloys. Our approach relaxes some of the commonly made assumptions concerning the evaluation of transition matrix elements, involves realistic models of the electronic band structure and the phonon spectra, and verifies the applicability of the Born approximation in treating alloy scattering. Our results for the homogeneous lifetime broadening of an electron at the bottom of the Γ valley combined with the inhomogeneous contributions obtained from Ref. 58 agree well with several sets of experimental data.

ACKNOWLEDGMENTS

We would like to thank H. Kalt, W. W. Rühle, and S. Logothetidis for stimulating discussions and access to their results before publication. C.G. acknowledges partial support of the Natural Sciences and Engineering Research Council of Canada.

*Present address: Division of Applied Sciences, Harvard University, Cambridge, MA 02138.

†Present address: IBM Research, P. O. Box 218, Yorktown Heights, NY 10598.

¹I. B. Gunn, IBM J. Res. Dev. **8**, 141 (1964).

²M. C. Nuss, D. H. Auston, and F. Capasso, Phys. Rev. Lett. **58**, 2355 (1987).

³M. Rinker, H. Kalt, and K. Köhler, Appl. Phys. Lett. **57**, 584 (1990); H. Kalt, A. L. Smirl, and T. F. Boggess, J. Appl. Phys. **65**, 294 (1988).

⁴D. L. Rode and P. A. Fedders, J. Appl. Phys. **54**, 6425 (1983).

⁵J. A. Kash, J. M. Hvam, J. C. Tsang, and T. F. Kuech, Phys. Rev. B **38**, 5776 (1988).

⁶O. K. Kim and W. G. Spitzer, J. Appl. Phys. **50**, 4362 (1979).

⁷N. Saint-Cricq, G. Landa, J. B. Renucci, I. Hardy, and A. Munoz-Yagne, J. Appl. Phys. **61**, 1206 (1987).

⁸S. Das Sarma, J. K. Kain, and R. Jalabert, Phys. Rev. B **41**, 3561 (1990).

⁹L. Pintschovius, J. A. Vergès, and M. Cardona, Phys. Rev. B **26**, 5658 (1982); M. Combescot, R. Combescot, and J. Bok, Europhys. Lett. **2**, 31 (1986).

¹⁰K. Bohnert, H. Kalt, A. L. Smirl, D. P. Norood, T. F. Boggess, and I. J. D'Haenens, Phys. Rev. Lett. **60**, 37 (1988).

¹¹R. W. Martin and J. L. Störmer, Solid State Commun. **22**, 523 (1977).

¹²A. Baldereschi, E. Hess, K. Maschke, H. Neumann, K. R. Schulze, and K. Unger, J. Phys. C **10**, 4709 (1977).

¹³S. J. Lee, T. S. Kwon, K. Nahm, and C. K. Kim, J. Phys. Con-

- dens. Matter **2**, 3253 (1990).
- ¹⁴Y. Fu, K. A. Chao, and R. Osorio, Phys. Rev. B **40**, 6417 (1989).
- ¹⁵Y. Shen and C. W. Myles, J. Phys. Chem. Solids **48**, 1173 (1987).
- ¹⁶L. Kleinman, Phys. Rev. B **35**, 3854 (1987).
- ¹⁷T. Ando, J. Phys. Soc. Jpn. **51**, 3893 (1982); **51**, 3900 (1982).
- ¹⁸P. K. Basu, Appl. Phys. Lett. **56**, 1110 (1990).
- ¹⁹P. Basa and B. Nag, Appl. Phys. Lett. **43**, 689 (1983).
- ²⁰J. W. Harrison and J. R. Hauser, Phys. Rev. B **13**, 5347 (1976); J. Appl. Phys. **47**, 292 (1976); **47**, 4712 (1976).
- ²¹J. Reggiani in *Hot Electron Transport in Semiconductors*, edited by L. Reggiani (Springer-Verlag, Berlin, 1985).
- ²²E. Caruthers and P. J. Lin-Chung, Phys. Rev. B **17**, 2705 (1978).
- ²³W. Andreoni and R. Car, Phys. Rev. B **21**, 3334 (1986).
- ²⁴W. E. Pickett, S. G. Louie, and M. L. Cohen, Phys. Rev. B **17**, 815 (1978).
- ²⁵G. Lehmann and M. Taut, Phys. Status Solidi B **54**, 469 (1972).
- ²⁶S. Adachi, J. Appl. Phys. **58**, R12 (1985).
- ²⁷E. M. Conwell, Solid State Phys. **9**, 149 (1967).
- ²⁸S. Zollner, S. Gopalan, and M. Cardona, SPIE Proc. **1282**, 78 (1980); J. Appl. Phys. **68**, 1682 (1990); S. Zollner, J. Kircher, M. Cardona, and S. Gopalan, Solid-State Electron. **32**, 1585 (1989).
- ²⁹A. S. Barker and A. Sievers, Rev. Mod. Phys. **47**, S1 (1975).
- ³⁰J. Leng, Y. Qian, P. Chen, and A. Madhukar, Solid State Commun. **69**, 311 (1989).
- ³¹B. Jusserand, D. Pacquet, and F. Mollot, Phys. Rev. Lett. **63**, 2397 (1989).
- ³²R. Bonneville, Phys. Rev. B **29**, 907 (1984).
- ³³P. Soven, Phys. Rev. **156**, 809 (1967).
- ³⁴D. W. Taylor, Phys. Rev. **156**, 1017 (1967).
- ³⁵K. Kunc and O. H. Nielsen, Comput. Phys. Commun. **17**, 413 (1979); K. Kunc and H. Bilz, Solid State Commun. **19**, 1027 (1976).
- ³⁶D. W. Taylor, Solid State Commun. **13**, 117 (1973).
- ³⁷K. C. Hass, B. Velický, and H. Ehrenreich, Phys. Rev. B **29**, 3697 (1984).
- ³⁸B. Strauch and D. Dorner, J. Phys. Condens. Matter **2**, 1457 (1990).
- ³⁹P. Giannozzi, S. de Gironcoli, P. Pavone, and S. Baroni, Phys. Rev. B **43**, 7231 (1991).
- ⁴⁰D. J. Mowbray, M. Cardona, and K. Ploog, Phys. Rev. B **43**, 1598 (1991).
- ⁴¹S. Baroni, S. de Gironcoli, and P. Giannozzi, in the *20th International Conference on the Physics of Semiconductors*, edited by E. M. Anastassakis and J. D. Joannopoulos (World Scientific, Singapore, 1990), Vol. 3, p. 1739.
- ⁴²J. A. Kash, S. S. Jha, and J. C. Tsang, Phys. Rev. Lett. **58**, 1869 (1987).
- ⁴³B. Jusserand and J. Sapriel, Phys. Rev. B **24**, 7194 (1981).
- ⁴⁴E. N. Economou and M. H. Cohen, Phys. Rev. Lett. **25**, 1445 (1970).
- ⁴⁵C. H. Grein and S. John, Phys. Rev. B **36**, 7457 (1987); **39**, 1140 (1989).
- ⁴⁶A. B. Chen and A. Sher, Phys. Rev. B **23**, 5360 (1981).
- ⁴⁷E. Merzbacher, *Quantum Mechanics*, 2nd ed. (Wiley, New York, 1970), p. 492.
- ⁴⁸R. J. Elliott, J. A. Krumhansl, and P. L. Leath, Rev. Mod. Phys. **46**, 465 (1974).
- ⁴⁹S. Krishnamurthy, M. A. Berding, A. Sher, and A. B. Chen, Phys. Rev. B **37**, 4254 (1988).
- ⁵⁰R. J. Lempert, K. C. Hass, and H. Ehrenreich, Phys. Rev. B **36**, 1111 (1987).
- ⁵¹H. Shiba, Prog. Theor. Phys. **46**, 77 (1971).
- ⁵²J. Kudrnovský and J. Mašek, Phys. Rev. B **31**, 6424 (1985).
- ⁵³Y. Shen and C. W. Myles, J. Phys. Chem. Solids **48**, 1173 (1987).
- ⁵⁴J. Klafter and J. Jortner, J. Chem. Phys. **68**, 1513 (1978).
- ⁵⁵S. Rudin and T. L. Reinecke, Phys. Rev. B **41**, 7713 (1990).
- ⁵⁶H. Kalt, W. W. Rühle, and K. Reimann, Solid-State Electron. **32**, 1819 (1989); H. Kalt, K. Reimann, M. Rinker, W. W. Rühle, and E. Bauser, in *20th International Conference on the Physics of Semiconductors*, edited by E. M. Anastassakis and J. D. Joannopoulos (World Scientific, Singapore, 1990), Vol. 3, p. 2498.
- ⁵⁷H. Kalt, W. W. Rühle, K. Reimann, M. Rinker, and E. Bauser, Phys. Rev. B **43**, 12364 (1991).
- ⁵⁸E. F. Schubert, E. O. Göbel, Y. Horikoshi, K. Ploog, and H. J. Queisser, Phys. Rev. B **30**, 813 (1984).
- ⁵⁹S. Logothetidis, M. Cardona, and C. Trallero-Giner, J. Appl. Phys. **67**, 4133 (1990); S. Logothetidis, M. Cardona, and M. Garriga, Phys. Rev. B **43**, 11950 (1991).
- ⁶⁰C. Trallero-Giner, V. O. Gavrilenko, and M. Cardona, Phys. Rev. B **40**, 1238 (1989).
- ⁶¹F. Yonezawa and K. Morigaki, Prog. Theor. Phys. Suppl. **53**, 1 (1973).
- ⁶²S. Sakai and T. Sugano, J. Fac. Eng., Univ. Tokyo **35**, 259 (1979).